Line node positions of the superconducting gap function of UPd_2Al_3

Peter Thalmeier[1] and David Parker[2]
[1]*Max Planck Institute for Chemical Physics of Solids, Nöthnitzer Strasse 40, 01187 Dresden, Germany*
[2]*US Naval Research Laboratory, 4555 Overlook Avenue SW, Washington, DC 20375, USA*
(Received 23 January 2009; revised manuscript received 12 March 2009; published 15 April 2009)

The field-angular oscillation of the magnetothermal conductivity is a powerful method for clarifying the gap symmetry of unconventional superconductors. It has been used successfully in Sr_2RuO_4, $CeCoIn_5$, and the cuprates, and has been applied to the heavy-fermion superconductor UPd_2Al_3. Despite this last application, however, there is still a controversy regarding the gap symmetry of UPd_2Al_3, with separate proposals for $\Delta(\mathbf{k})=\Delta_0 \cos k_z$ and $\Delta(\mathbf{k})=\Delta_0 \cos 2k_z$ in the literature *from analyzing the same thermal-conductivity data*. In this paper we systematically study this important issue and show conclusively from all available experimental evidence that, consistent with theoretical grounds, $\Delta_0 \cos k_z$ is the actual gap function of UPd_2Al_3.

DOI: 10.1103/PhysRevB.79.134514 PACS number(s): 74.20.Rp, 74.25.Fy, 74.70.Tx

I. INTRODUCTION

In unconventional superconductors the gap function or superconducting order parameter (OP) transforms as a nontrivial representation of the symmetry group of the crystal. The latter is comprised of point-group and translation group operations as well as gauge transformations and time-reversal operation.[1] Because superconductivity implies off-diagonal long-range order,[2] the order parameter does not correspond to the density of a physical observable. Therefore it cannot be observed directly and its symmetry is notoriously hard to determine. The main established methods are the low-temperature behavior of thermodynamic quantities, NMR Knight shift and relaxation rate,[3] and more recently the field-angle-resolved magnetothermal transport[3,4] and feedback spin-resonance effects in inelastic neutron scattering (INS).[5,6] These methods cannot give a precise determination of $\Delta(\mathbf{k})$ everywhere on the Fermi surface (FS) but at best the position and orientation (with respect to k_i, $i=x,y,z$ axes) of node lines and points where $\Delta(\mathbf{k})$ vanishes.[3,4]

The latter method has recently been quite successful in determination of nodal positions in the heavy-fermion superconductors such as UPd_2Al_3,[7–10] $CeCu_2Si_2$,[11] and $CeCoIn_5$.[12] The nodal positions may be determined when a feedback resonance in the superconducting state is observed at a position $\mathbf{Q}$ with an energy $\omega_r < 2\Delta_0$. It has appreciable intensity only when the BCS coherence factors at $\mathbf{Q}$ are large which necessarily requires the condition $\Delta(\mathbf{k}) = -\Delta(\mathbf{k}+\mathbf{Q})$ to be fulfilled. This condition is very selective for the superconducting order parameter and almost as strong as a Bragg condition for magnetic order parameters. Indeed in $CeCu_2Si_2$ the feedback resonance in the superconducting sample is replaced by a spin-density wave (SDW) Bragg peak at the same (incommensurate) wave vector for samples with different stoichiometry. A similar observation is made in Ir-doped $CeCoIn_5$ which develops incommensurate magnetic order[13] at a wave vector $\mathbf{Q}_{SDW}$ which has the same in-plane components as $\mathbf{Q}$ where the undoped superconducting compound displays the feedback resonance.[12]

The method of field-angle-resolved magnetothermal conductivity[4] is based on Volovik's observation[14] that, in the vortex phase of unconventional superconductors with line nodes, quasiparticle states may exist outside the vortex cores. They can carry a heat current perpendicular to the vortices whose magnitude depends on the orientation of the field with respect to the node lines. When the field orientation is continuously rotated in a crystal plane, two situations may occur (Fig. 1): if the field direction crosses the nodal plane (left) typical angular oscillations in the low-T thermal conductivity (heat current $\perp$ vortex direction) appear. Field-angular oscillations of this type are also observed in the low-T specific heat. If the field is rotated within the nodal plane (right), no oscillations are observed. By using different field-rotation planes in the experiment, one may thus infer the orientation of the nodal plane with respect to the crystal axes. Fortunately, this determination does not depend on any quantitative analysis but may be directly obtained by inspection of experimental results. On the other hand it is not obvious at which position perpendicular to this plane (along the z axis in Fig. 1) the node lines are located. To decide this issue a detailed theoretical analysis for the possible model gap functions is required.

This is different from the INS feedback method which gives both the nodal plane and the position of nodes along the perpendicular coordinate. INS was able to identify the $d_{x^2-y^2}$ gap function in $CeCoIn_5$ uniquely[5,12] whereas specific heat and thermal-conductivity results only determined the nodal plane as perpendicular to the tetragonal ab plane but at first were not able to distinguish between the $d_{x^2-y^2}$ (Ref. 15)

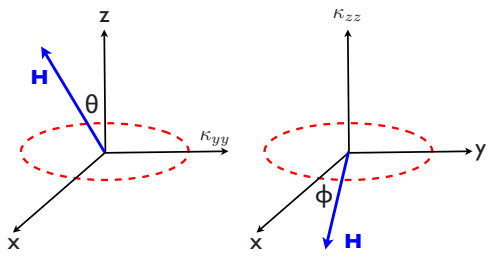

FIG. 1. (Color online) Schematic illustration of geometry in field-angle-resolved magnetothermal-conductivity experiments. In both configurations [left (right): **H** rotation in xz (xy) plane] the heat current is perpendicular to the field-rotation plane. The node line of the order parameter is indicated by the dashed line. For this geometry $\kappa_{yy}(\theta)$ shows oscillations while $\kappa_{zz}(\phi)$ does not.

and d_{xy} (Ref. 16) states. For further discussion of this issue, see Ref. 17.

In this work we consider exclusively the heavy-fermion superconductor UPd_2Al_3.[18] An extended body of experimental and theoretical work has accumulated on this compound. Despite this effort there is still no consensus on the symmetry of $\Delta(\mathbf{k})$ as seen from Ref. 19 [i.f. denoted as (I)], Ref. 20 [i.f. denoted as (II)], and also in Ref. 21. This compound is unique because it is the only heavy-fermion system where the nonphononic nature of pairing has been confirmed.[8,22,23] Therefore it is important to clarify the issue of gap symmetry. Before we enter this discussion we briefly summarize the basic physical properties of UPd_2Al_3. For more details we refer to Ref. 3. This moderate heavy-fermion compound ($\gamma = 140$ mJ/mol K^2) with D_{6h} symmetry orders antiferromagnetically at $T_N=14.3$ K with a sizable moment $\mu=0.85\mu_B$. The easy-plane antiferromagnetic (AF) structure consists of ferromagnetic (FM) planes stacked along the c axis with alternating moments, i.e., a commensurate $\mathbf{Q}=(0,0,\frac{\pi}{c})$ with $c=4.185$ Å denoting the lattice constant of the *chemical* unit cell along the hexagonal axis. Because $T_c=1.8$ K is much smaller than T_N the AF order will not be influenced by the onset of superconductivity. On the other hand the large moment staggered magnetization leads to an exchange splitting and reconstruction of conduction-electron bands which have to be considered in the AF Brillouin zone with zone boundaries (Bragg planes) at $k_z=\pm\frac{\pi}{2c}$.

In Sec. II we introduce microscopic models for the $5f$ electronic structure and the associated pairing mechanism. This section will be kept short because an extensive literature about this topic exists.[3,23–26] The INS and magnetotransport experiments from which the controversy about the gap symmetry appeared will be discussed in detail in Sec. III. In the main Sec. V we will discuss the proper interpretation of the magnetothermal-conductivity results and compare the resulting gap function with the INS results. Finally, Sec. VII gives the conclusions.

II. ELECTRONIC STRUCTURE AND PAIRING MODELS

Now we briefly discuss the main microscopic theoretical models put forward to explain the heavy-fermion character as well as the magnetic order and superconductivity. The $5f$ states in UPd_2Al_3 have a dual character: they are partly localized and partly itinerant.[8,24] The localized $5f$ electrons, with two low lying crystalline electric field (CEF) split singlets about $\Delta_{CEF}\simeq 6$ meV apart, lead to an induced moment magnetism.[27] The conduction electrons have a FS whose main sheet is a corrugated cylinder which is aligned with the c axis[24,28] and has a FS area corrugation $\sim 25\%$. We stress that the FS cylinder is located in the magnetic Brillouin zone and is terminated by the AF Bragg planes (Fig. 4). The on-site exchange interaction between both components leads to two major effects:[23,24] a mass renormalization to form heavy quasiparticles with an enhancement of $m^*/m_b\sim 10$ (m_b =band mass) and an effective intersite exchange interaction between the localized singlet-singlet CEF excitations. The latter causes the sharp CEF excitation at Δ_{CEF} to broaden into a band $\omega_E(\mathbf{q})$ of magnetic excitons which now extends from 1–8 meV (Ref. 27) and has a pronounced minimum at the AF wave vector $\mathbf{Q}$. For $T\ll\Delta$ they are bosonic excitations whose virtual exchange processes with conduction electrons mediate an effective pairing interaction between them which is responsible for superconductivity in UPd_2Al_3.[23]

The absolute value of the effective pairing interaction has a pronounced maximum at $\mathbf{Q}$ due to the minimum of $\omega_E(\mathbf{q})$. As in single-component itinerant spin-fluctuation theories,[29] one then expects that the superconducting gap function should show a sign change under translation $\mathbf{k}\rightarrow\mathbf{k}+\mathbf{Q}$, i.e., $\Delta(\mathbf{k}) = -\Delta(\mathbf{k}+\mathbf{Q})$. A linearized solution of Eliashberg equations indeed leads to the most favorable (with largest T_c) singlet gap function $\Delta(\mathbf{k})=\Delta_0\cos k_z$.[23] Triplet gap functions are not discussed here because the observation of a sizable Knight shift[30] gives a strong preference to the singlet state. The gap function $\Delta(\mathbf{k})=\Delta_0\cos 2k_z$ of Ref. 20 is not a solution with positive T_c in this model. In fact it has the property $\Delta(\mathbf{k})=\Delta(\mathbf{k}+\mathbf{Q})$ and therefore cannot take advantage of a pairing interaction peaked at $\mathbf{Q}$. A similar observation was made in Ref. 25 using a one-component itinerant spin-fluctuation model for UPd_2Al_3. The self-consistently determined gap function obtained by solving the Eliashberg equations was found to resemble very closely the simple $\Delta(\mathbf{k})=\Delta_0\cos k_z$ in shape. Thus from the point of view of microscopic models there is no reason to expect a gap function $\Delta(\mathbf{k})=\Delta_0\cos 2k_z$.

III. RESULTS ON GAP SYMMETRY DETERMINATION

In a series of INS results it was found that UPd_2Al_3 is the first example of a heavy-fermion superconductor with a resonant superconducting feedback effect:[8,9,31] Above T_c a broad INS peak at $\mathbf{Q}=(0,0,\frac{\pi}{c})$ appears at the energy $\omega_E(\mathbf{Q})\simeq 1.5$ meV. At $T=0.15$ K$\ll T_c$ an additional sharp inelastic resonance at $\omega_r\simeq 0.35$ meV appears which may be interpreted as a split-off satellite of $\omega_E(\mathbf{Q})$. It is due to a feedback effect of the superconducting order parameter on the pair-forming magnetic exciton boson. The renormalized exciton mode and the resonance satellite are solutions of Dyson's equation

$$\omega^2=\omega_E^2(\mathbf{q})-2g^2\Delta_{CEF}\chi_0(\mathbf{q},\omega), \tag{1}$$

where Δ_{CEF} is the bare CEF splitting and g is the electron-exciton coupling constant.[10] The second term describes the renormalization of the exciton by particle-hole excitations. In the normal state $\chi_0(\mathbf{q},\omega)$ shows little frequency dependence and only a constant shift of ω_E occurs. However, below T_c the particle-hole-excitation spectrum is modified due to the gap opening which leads to a pronounced frequency dependence of $\chi_0(\mathbf{Q},\omega)$ around $\omega\simeq 2\Delta_0$ (Δ_0=gap amplitude). This superconducting feedback on the conduction-electron response and hence on the renormalized boson frequency [Eq. (1)] leads to the appearance of an additional resonance as shown in detail in a microscopic model.[10] The resonance exists only in the close vicinity of the wave vector $\mathbf{Q}$ and shows an upward dispersion following that of the renormalized exciton. The feedback resonance appears only when the superconducting coherence factors in the electronic response function are large. This necessarily implies that the condition

$\Delta(\mathbf{k}+\mathbf{Q})=-\Delta(\mathbf{k})$ for the gap function must be fulfilled. The resonance condition for the superconducting order parameter has roughly a similar meaning as that of the Bragg condition for a magnetic order parameter although at finite instead of zero energy transfer, respectively. Therefore it was realized rather early[8,31,32] that the simplest type of gap function compatible with the resonance condition can be represented as Fourier series with odd harmonics where $\Delta(\mathbf{k})=\Delta_0 \cos k_z$ is the first harmonic contribution. On the other hand the complementary even gap functions such as $\Delta(\mathbf{k})=\Delta_0 \cos 2k_z$ which fulfill $\Delta(\mathbf{k}+\mathbf{Q})=\Delta(\mathbf{k})$ have to be strictly excluded when a resonance at $\mathbf{Q}$ like in UPd_2Al_3 is observed. This issue is discussed further in Sec. IV. Thus the feedback resonance condition in the superconducting state leads to the same gap function[10] $\Delta_0 \cos k_z$ as the theoretical calculations which use a magnetic excitation spectrum observed in the normal state. This shows that the pairing model and the theory of the resonance state are fully consistent.

This conclusion became even more convincing when the second important technique, field-angle-resolved magnetothermal conductivity, was used to investigate the gap symmetry[19] (I). Using two configurations (Fig. 1) with (i) heat current $\|\hat{\mathbf{y}}$ and rotating $\mathbf{H}$ in the xz plane with polar angle θ, and (ii) heat current $\|\hat{\mathbf{z}}$ and rotating $\mathbf{H}$ in the xy plane with azimuthal angle ϕ, the thermal conductivities $\kappa_{yy}(\theta)$ and $\kappa_{zz}(\phi)$ were measured. It was found that at low T the former shows a pronounced twofold oscillation whereas the latter shows none. Without any analysis it can then be concluded that the node lines of the order parameter must be parallel to the hexagonal ab (xy) plane. However no detailed calculations were performed in (I) to find out at what position $\chi=ck_z$ these lines are located. Rather it was argued qualitatively, based on the proper cylindrical Fermi-surface geometry and the Doppler-shift (DS) theory for transport coefficients. It was concluded that $\Delta_0 \cos k_z$ leads to the proper twofold oscillation of $\kappa_{yy}(\theta)$ while $\Delta_0 \cos 2k_z$ would lead to a fourfold oscillation in contradiction to experiment (see Fig. 4 in Ref. 19). This conjecture was later fully confirmed by a numerical evaluation of Doppler-shift based thermal conductivity in the unitary limit.[21] So finally a complete agreement on the gap symmetry $\Delta_0 \cos k_z$ of UPd_2Al_3 based on INS results, microscopic theories, and magnetothermal-conductivity results was achieved.

However this consensus was called in question later in[20] (II) on the basis of an approximate analytical Doppler-shift treatment of thermal transport. It was proposed that *only* $\Delta_0 \cos 2k_z$ was compatible with thermal-conductivity results opposite to INS results which rule out this gap function. This ambiguity has to date not been resolved. Since UPd_2Al_3 is of pivotal importance for understanding unconventional heavy-fermion superconductivity, we reconsider this case here and propose how to resolve the issue. Therefore in the present work the magnetotransport is discussed within the same theoretical approach as was used in (II).

IV. SYMMETRY CLASSIFICATION AND COEXISTENCE WITH ANTIFERROMAGNETISM

Before we discuss the magnetothermal conductivity it is appropriate to understand the symmetry classifications of both gap function candidates. We restrict our analysis to gap functions that depend only on k_z since the node lines have been found to be parallel to the ab plane. Furthermore the effective pairing interaction peaks at a wave vector $\mathbf{Q}$ parallel to $k_z\hat{\mathbf{z}}$. Such gap functions belong to the A_{1g} representation with respect to the point group D_{6h}. We also consider only singlet pairing, i.e., even under inversion. In this restricted class only the translation along the z axis remains as a symmetry operation. In real space the primitive translation vector along z is $2c\hat{\mathbf{z}}$ because of the doubling of the AF unit cell. This is the proper cell since $T_N \gg T_c$ and the exchange splitting of conduction electrons is much larger than Δ_0. In reciprocal space the primitive translation is therefore $\mathbf{Q}=\frac{\pi}{c}\hat{\mathbf{z}}$. There are two possible classes of gap functions classified by their transformation under translation by $\mathbf{Q}$: (class A) $\Delta(\mathbf{k}+\mathbf{Q})=\Delta(\mathbf{k})$ and (class B) $\Delta(\mathbf{k}+\mathbf{Q})=-\Delta(\mathbf{k})$. Both are invariant under all other symmetry elements. Therefore class A is of a fully symmetric "extended s-wave" type whereas class B behaves nontrivially under translation by $\mathbf{Q}$ and therefore is a truly unconventional gap function. These gap functions may be expanded in harmonics according to

$$\text{class A:}\quad \Delta(\mathbf{k})=\sum_{n\geq 1,\text{odd}} \Delta_0^{(n)} \cos nk_z \simeq \Delta_0^{(1)} \cos ck_z,$$

$$\text{class B:}\quad \Delta(\mathbf{k})=\sum_{n\geq 2,\text{even}} \Delta_0^{(n)} \cos nk_z \simeq \Delta_0^{(0)}+\Delta_0^{(2)} \cos 2ck_z. \tag{2}$$

In the real-space representation $\Delta_0^{(n)}$ is the pairing amplitude of a conduction state $|0,\uparrow\rangle$ in hexagonal layer 0 with a state $|n,\downarrow\rangle$ in layer n. Since the hexagonal layers have FM order stacked antiferromagnetically along c, this has important implications for the coexistence with AF order discussed below.

The nodal structure of class A and B gap functions shows an important difference: the unconventional class B has node lines at $\chi=ck_z=\pm\frac{\pi}{2}$ lying in the Bragg planes of the AF Brillouin zone. These node lines are symmetry protected due to the sign change in the gap under translation by $\mathbf{Q}$, i.e., they are independent of the higher harmonic coefficients (since each odd harmonic vanishes at the Bragg planes). We can make the reasonable assumption that the higher harmonic amplitudes decay quickly with order since the effective pairing interaction which is determined by the exciton dispersion along c also shows only a pronounced harmonic with $n=1$. Then the node line in the Bragg plane which is a *symmetry plane* will be the only one and will be independent of the details of the interaction models.

The situation is quite different for class B. First of all, none of the even harmonics can be expected to have an appreciable effective pairing potential for $n=0$ or $n=2$ because, for the magnetic exciton mechanism, the former will always be repulsive and the latter is not dominant in the exciton dispersion. If, nonetheless, we assume that $\Delta_0^{(2)}$ is the dominant gap amplitude, then inevitably $\Delta_0^{(0)}$ will also be induced because these gap functions belong to the same symmetry class B. Therefore the minimum model for class A (discarding higher harmonics with $n\geq 4$) is $\Delta(\mathbf{k})=\Delta_0^{(0)}+\Delta_0^{(2)} \cos 2k_z$. When $n=2$ is the primary OP and $n=0$ is induced we will

have $\Delta_0^{(0)} < \Delta_0^{(2)}$, and this order parameter has node lines at $\chi = ck_z = \pm\frac{\pi}{4} \pm \tan^{-1}(\Delta_0^{(0)}/\Delta_0^{(2)})$. These nodal planes (even if $\Delta_0^{(0)}=0$) are *nonsymmetry planes* of the hexagonal lattice. They are not protected by symmetry requirements, and their position depends on the amplitude ratio of $n=0$ and $n=2$. Therefore fixing them at $\chi=\pi/4c$ as in (II), i.e., assuming $\Delta_0^{(0)}=0$ is arbitrary. Even if we accept this as a hypothesis we should keep in mind that all known heavy-fermion superconductors (and in fact all known unconventional superconductors with inversion symmetry) have node lines within *symmetry* planes.

Let us nevertheless accept class B as a candidate gap function for the moment. There is another important aspect which one has to keep in mind. The superconducting state must be able to coexist deeply inside an AF phase that has an appreciable staggered moment ($\mu=0.85\mu_B/U$). This problem has been discussed by Shimahara[26] and for clarity we repeat here some of his arguments. Since the AF structure consists of FM hexagonal layers stacked in an alternating manner along c, it is natural to consider the pairing in c direction in real space as interlayer pairing with a singlet amplitude $\Psi_{ij}^{(s)} = \frac{1}{\sqrt{2}}(a_{i\uparrow}b_{j\downarrow} - a_{i\downarrow}b_{j\uparrow})$. Here i,j denote the sites in each layer and a or b denote layers with opposite moment or molecular field $h_{\mathrm{MF}}^a = -h_{\mathrm{MF}}^b$. This leads to a different size of the Fermi wave vectors $k_{F\sigma}^{a,b}$ in a,b type layers for electrons with given spin σ. The class A state corresponds to singlet (antisymmetrized opposite spin) pairing in adjacent (nearest-neighbor) a,b layers which have also opposite ordered moments (molecular fields). Therefore the Fermi radii will be equal, i.e., $k_{F\uparrow}^a = k_{F\downarrow}^b$. This means that class A superconductivity is easily coexistent with AF order in UPd_2Al_3.[26] On the other hand a class B state corresponds to in-plane a-a and interplane (next-nearest-neighbor) a-a' pairings. In both cases the ordered moments and molecular fields will be equal; however the paired singlet spins are opposite. Therefore $k_{F\uparrow}^a \neq k_{F\downarrow}^a$ and $k_{F\uparrow}^a \neq k_{F\downarrow}^{a'}$. The corresponding effective spin splitting of such states at the AF zone boundary is estimated to be of the order $\Delta_{\mathrm{ex}} \simeq 50-100$ meV.[10,23] This corresponds to an AF molecular field of $h_{\mathrm{MF}} \simeq 4.4-8.8\times 10^2$ T which is two orders of magnitude larger than the nominal BCS Pauli limiting field $H_P = \Delta_0/\sqrt{2}\mu_B \simeq 3.3$ T. Therefore class B pairing states are strongly suppressed by AF order of UPd_2Al_3.

Together the symmetry analysis and AF coexistence conditions make it already abundantly clear that a class B gap function such as $\Delta_0 \cos 2k_z$ is a most unlikely candidate. However, it is important to analyze the thermal-conductivity data whose analysis led to its proposal, in order to elucidate the source of the discrepancy, as this has a bearing on future magnetothermal-conductivity analyses.

V. MAGNETOTHERMAL CONDUCTIVITY

The divergent conclusions on the order-parameter symmetry in UPd_2Al_3 arose from different interpretations of the field-angle-resolved magnetothermal conductivity first presented in (I) and later discussed in (II) where the former proposed class A and the latter proposed class B gap function were realized. In both works the arguments are based on the simple Doppler-shift approach.[4,33,34] For the sake of comparison the same method will be used here.

The method is based on an observation by Volovik[14] that in the vortex phase of an unconventional superconductor quasiparticle states exist outside the vortex cores which can carry a heat current. They also lead to a residual zero energy density of states (ZEDOS) $N(0,\mathbf{H})$ whose value depends on the field direction with respect to the orientation of the node lines. Therefore rotation of the field may lead to an oscillatory behavior of the thermal conductivity and also the specific heat which contain information on the nodal structure of $\Delta(\mathbf{k})$.

In this experimental method pioneered by Y. Matsuda *et al.* (for a review, see Refs. 3 and 4) the thermal conductivity $\kappa_{\alpha\alpha}(\mathbf{H})$ is measured at temperatures $T \ll T_c$ where the magnetic field $\mathbf{H}$ is rotated in a symmetry plane of the crystal. Ideally the heat current $\mathbf{j_Q}$ should be perpendicular to the field-rotation plane. Thus $\kappa_{yy}(\theta)$ corresponds to field rotating in the xz plane with θ denoting the polar field angle from the z axis. Likewise $\kappa_{zz}(\phi)$ corresponds to field rotation in the xy plane with ϕ denoting the azimuthal field angle from the x axis; see Fig. 1 for an illustration. The main virtue of the method is its ability to determine the orientation of node lines in $\mathbf{k}$ space, i.e., whether such lines are parallel or perpendicular to symmetry axis, it may be determined without any calculation by pure inspection of the oscillatory behavior of $\kappa_{\alpha\alpha}(\mathbf{H})$ under various geometries. For example, in UPd_2Al_3 the experiment[19] observed oscillations in $\kappa_{yy}(\theta)$ but not in $\kappa_{zz}(\phi)$. From the geometrical arrangement in Fig. 1 it is obvious without further analysis that in this case the node lines must lie within the hexagonal ab (k_xk_y) plane. However, to determine at which position $\chi=ck_z$ along the hexagonal axis, these lines are located demands a detailed theoretical analysis and this has indeed led to different proposals for the node line position in UPd_2Al_3.

A. Doppler-shift expressions for the thermal conductivity

In the independent (single) vortex approach which is valid at fields sufficiently smaller than H_{c2}, the transport coefficients are expressed in terms of averaged transport integrals containing the Doppler shift of quasiparticle energies. Normalized to the maximum gap it is given by

$$x(\mathbf{k},\mathbf{r}) = (\mathbf{p}\cdot\mathbf{v}_s)/\Delta_0 = (m^*\mathbf{v}\cdot\mathbf{v}_s)/\Delta_0, \tag{3}$$

where $\mathbf{p}(\mathbf{k})$, $\mathbf{v}(\mathbf{k})$, and m^* are quasiparticle momentum, velocity, and effective mass, respectively. Furthermore $\mathbf{v}_s(\mathbf{r})$ is the superfluid velocity around the vortex centered at $\mathbf{r}=0$. The averaging in transport integrals has to be carried out over the Fermi surface ($\mathbf{k}$) and with respect to the position ($\mathbf{r}$) from the vortex center. For our present purpose we use the simplest possible approximation as, e.g., in Refs. 33 and 34. Firstly it is assumed that the condition $\Gamma \ll \langle|x|\rangle\Delta_0$ for the superclean limit is fulfilled where the ZEDOS is dominated by the Doppler shift and the influence of the scattering rate Γ can be neglected. Here $\langle\ldots\rangle$ denotes both averages over Fermi surface and vortex coordinate.[21,33,34] Secondly the averaging over the Fermi surface is approximated by one over the node line which gives the dominant contribution. This

approximation is sufficient if one only wants to describe qualitatively the angular oscillations; however it is too crude to give the proper amplitude of the oscillation. Within the superclean limit this was done by a fully numerical calculation of transport integrals[21] and it was found that the oscillation amplitude is of the order of a percent of the normal-state conductivity κ_n which is indeed the experimental scale of the oscillations.

In Refs. 20 and 34 a simple ellipsoid Fermi surface centered at the Γ (0,0,0) point is used for the calculations. Its uniaxial anisotropy parameter $\alpha=(v_c/v_a)^2$ is determined by the Fermi velocities along a and c axes. This is the only FS parameter that enters the calculation. The absolute size of the FS is irrelevant as long as it is cut by the node line of the gap function (see Fig. 4). We will later discuss to which extent such simplifying FS assumptions can be made. According to Refs. 20 and 34 we then have, for the ZEDOS and thermal conductivity, respectively,

$$\frac{N(\theta)}{N_0} = g(\theta) = \frac{2}{\pi}\frac{v_a\sqrt{eH}}{\Delta_0} I(\theta),$$

$$\frac{\kappa_{yy}(\theta)}{\kappa_{yy}^n} = \frac{2}{\pi}\frac{v_a^2(eH)}{\Delta_0^2} I(\theta) I_{yy}(\theta), \tag{4}$$

where N_0 and κ_{yy}^n are the normal-state DOS and thermal conductivity. The ZEDOS integral $I(\theta)$ and the transport integral $I_{yy}(\theta)$ have to be taken around the node line in the hexagonal plane according to

$$I(\theta) = (\cos^2\theta + \alpha \sin^2\theta)^{1/4}\frac{1}{\pi}\int_0^\pi d\phi \sqrt{L(\theta,\phi,\alpha\sin^2\chi_0)},$$

$$I_{yy}(\theta) = (\cos^2\theta + \alpha\sin^2\theta)^{1/4}\frac{2}{\pi}\int_0^\pi d\phi \sin^2\phi \sqrt{L(\theta,\phi,\alpha\sin^2\chi_0)}, \tag{5}$$

where $\sin\phi = v_F^y/v_F$ is the (normalized) quasiparticle velocity component along the direction of the heat current. Furthermore the integrand is the absolute value of the Doppler shift already averaged over the vortex coordinates. In addition Eq. (5) contains the averaging over the node line azimuthal angle ϕ. The function under the square root is given by[20,34]

$$L(\theta,\phi,\alpha\sin^2\chi_0) = \cos^2\theta + \sin^2\theta(\sin^2\phi + \alpha\sin^2\chi) + \sqrt{\alpha}\sin\chi\cos\phi\sin(2\theta), \tag{6}$$

where $\chi = ck_z$ is the position of the node line along the c axis, which differs in the two gap models discussed here. The expression for κ_{yy} in Eq. (4) has a simple physical meaning: with an additional factorization of $I_{yy}(\theta)$ we obtain approximately

$$\kappa_{yy} = \langle v_y^2\rangle C_s \tau_{\rm tr},$$

$$C_s/C_n = g(\theta); \quad \tau_{\rm tr}/\tau = \pi g(\theta), \tag{7}$$

where $C_n=(\pi^2/3)N_0T$ is the normal state and C_s is the superconducting state specific heat, respectively. Furthermore $\tau_{\rm tr}$ is the transport lifetime in the unitary scattering limit with $\tau=1/2\Gamma$, where Γ is the impurity scattering rate. The reduced ZEDOS $g(\theta)$ is defined in Eq. (4). The approximate expression in Eq. (7) which was also implicitly used in (II) is simply the kinetic thermal transport formula. The field-angular dependence of $\kappa_{yy}(\theta)$ in this approximation is entirely determined by that of the field induced ZEDOS of the heat carrying quasiparticles given in Eq. (4).

B. Numerical results for transport integrals and relation to Fermi-surface geometry

In the present model the field-angular dependence is influenced by two parameters: the nodal position χ of the gap function candidate and the overall quasiparticle velocity anisotropy α. Since the Fermi surface is described by a simple ellipsoid, α is to be interpreted as an averaged quantity over the real Fermi-surface sheets. This may in principle be obtained from the anisotropy of the upper critical-field slope.[21,35,36] However experimentally the situation is not so clear. Upper critical-field data from epitaxially grown thin films[37] suggest $\alpha=0.69$. This value was used in previous discussions.[20,21] However it may be unreliable due to special thin-film effects such as substrate strain, etc. On the other hand the first measurements from bulk single crystals lead to $\alpha=0.85$.[38] In a recent review[39] a value $\alpha=1$, i.e., isotropic upper critical-field slope, is suggested. Here we take the intermediate value $\alpha=0.85$. Our fundamental conclusions do not depend on this value. Generally speaking, when α becomes larger the difference in the angular dependence of thermal conductivity for the two gap functions discussed here becomes more pronounced.

To determine the angular dependence of $\kappa_{yy}(\theta)$, it is necessary to carry out the Doppler-shift integration around the node line in Eq. (5) in a precise way. In (I) qualitative arguments only were given and in (II) these integrals were approximated by replacing Eq. (5) with

$$\tilde{I}(\theta) = (\cos^2\theta + \alpha\sin^2\theta)^{1/4}\frac{1}{\pi}\sqrt{\int_0^\pi d\phi L(\theta,\phi,\alpha\sin^2\chi_0)}, \tag{8}$$

and similarly for $\tilde{I}_{yy}(\theta)$, i.e., the node line averaging over ϕ is performed under the square root instead of outside. However it turns out that, for reasonably large α corresponding to UPd_2Al_3, this causes a problem. This can be seen from a comparison of thermal conductivities in Eq. (4) using the exact numerically integrated $I(\theta)$, $I_{yy}(\theta)$ of Eq. (5) or the approximations $\tilde{I}(\theta)$, $\tilde{I}_{yy}(\theta)$ in Eq (8). The comparison is shown in Fig. 2 for the B-class gap function $\Delta_0\cos 2k_z$. It is obvious that the approximation of Eq. (8) used in (II) misses higher harmonics in θ which are present in the exact DS integrals of Eq. (5). We conclude that the approximate $\tilde{I}(\theta)$ and $\tilde{I}_{yy}(\theta)$ of Eq. (8) leads to a twofold (dashed line) instead of the proper fourfold (full line) thermal-conductivity oscil-

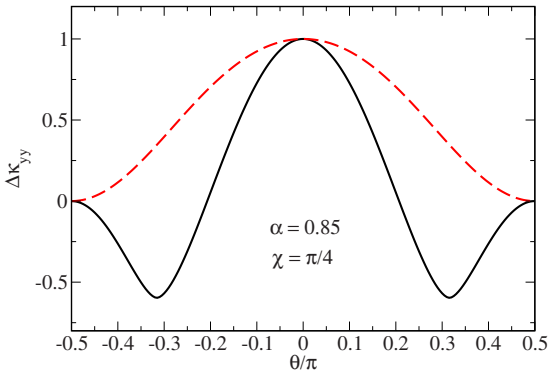

FIG. 2. (Color online) A comparison of normalized thermal conductivity [Eq. (9)] for $\Delta_0 \cos 2k_z$ gap function from an exact numerical Doppler-shift integration (full line) according to Eqs. (4)–(6) and an analytical approximation according to Eq. (8) used also in Eq. (16) of Ref. 20 (II) (dashed line). The latter is inadequate because it leads to the wrong periodicity as compared to the exact numerical integration.

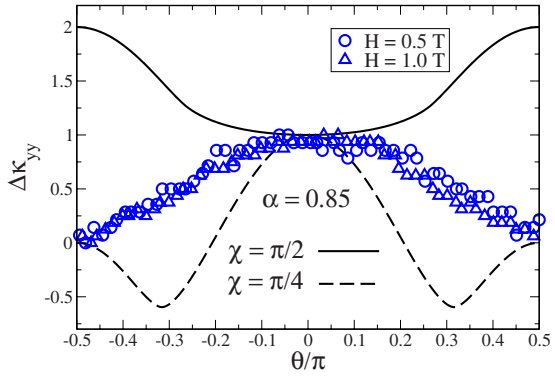

FIG. 3. (Color online) A comparison of normalized thermal-conductivity calculations for $\Delta_0 \cos k_z$ (full line, $\chi=\pi/2$) and $\Delta_0 \cos 2k_z$ (dashed line, $\chi=\pi/4$) using the exact numerical integration of Doppler-shift expressions [Eqs. (4)–(6)]. Here the Γ (0,0,0)-centered Fermi-surface model of Fig. 4 (left) is used. The symbols are the experimental results from Watanabe *et al.* (Ref. 19) (I). Both gap models are in disagreement with the experimental results.

lation for this gap function (Fig. 2). Therefore in the following for comparing with experimental results we will only use the exact numerical DS integrals $I(\theta)$ and $I_{yy}(\theta)$ of Eq. (5). Note that in Fig. 2 and later figures we use the subtracted and normalized thermal conductivity

$$\Delta\kappa_{yy}(\theta) = \frac{\kappa_{yy}(\theta) - \kappa\left(\frac{\pi}{2}\right)}{\kappa_{yy}(0) - \kappa\left(\frac{\pi}{2}\right)} \quad \text{for} \quad \kappa_{yy}(0) > \kappa\left(\frac{\pi}{2}\right),$$

$$\Delta\kappa_{yy}(\theta) = \frac{\kappa_{yy}(0) - \kappa(\theta)}{\kappa_{yy}(0) - \kappa\left(\frac{\pi}{2}\right)} + 1 \quad \text{for} \quad \kappa_{yy}(0) < \kappa\left(\frac{\pi}{2}\right). \tag{9}$$

Thus $\Delta\kappa_{yy}(0)$ is always normalized to one and $\Delta\kappa_{yy}(\frac{\pi}{2})$ is always normalized to zero (two) depending on whether $\Delta\kappa_{yy}(\theta)$ decreases or increases away from $\theta=0$. The same normalization will be chosen for the experimental data of (I). The latter are now compared with theoretical results for both class A and B order parameters $\Delta_0 \cos k_z$ and $\Delta_0 \cos 2k_z$ using the exact numerical DS integration in Eq. (5). This comparison is shown in Fig. 3. It is obvious that none of the models agrees with the experimental field-angle dependence. As already mentioned, for the class B gap function with node position $\chi=\pi/2$ (dashed line), the wrong oscillation period is obtained. On the other hand class A gap function (full line) leads to the proper period but the wrong sign, i.e., $\Delta\kappa_{yy}(\theta)$ increases with increasing θ in contrast to the experimental values. The wrong period for class B was not noticed in (II) because the approximate DS integration as shown in Fig. 2 has been used while the wrong sign for class A was also noticed. Therefore it was concluded in (II) that $\Delta_0 \cos k_z$ (class A) is rejected by experiment and class B is confirmed. The present exact numerical analysis of DS integrals given in Fig. 3 however shows that no such conclusion can be drawn: both gap functions (classes A and B) in this calculation fail to explain the experimental data.

This is a surprising result, especially considering the strong arguments for the correctness of class A from other evidence explained in previous sections. Therefore one has to inquire about the soundness of the calculation described above. For both gap functions the problem is the upturn in $\Delta\kappa_{yy}(\theta)$ for increasing θ, starting immediately for class A and above $\theta=0.3\pi$ for class B. The origin of this problem can be spotted in the DS integrand of Eq. (6). The term $\sim\alpha \sin^2\theta \sin^2\chi$ leads to a large increase in the integrand for large θ especially when $\chi=\pi/2$ (class A). This overcompensates the prefactor in Eq. (5) and causes the increase in $\Delta\kappa_{yy}(\theta)$ for large θ.

This term is $\sim v_c^2$, the square of the c component of the Fermi velocity which is surprising for the following reason: for $\chi=\pi/2$ (class A) the node line is lying within the AF zone-boundary Bragg plane. In such a case Bloch's theorem strictly requires that the quasiparticle velocity $\mathbf{v}$ is *parallel* to the Bragg plane, i.e., there should be no term with a v_c component of the velocity in the case $\chi=\pi/2$. The reason why in the present model it appears nevertheless is illustrated in Fig. 4. The underlying Fermi-surface (FS) model used in (II) is a Γ (0,0,0) centered elliptical Fermi surface with a single anisotropy parameter $\alpha=(v_c/v_a)^2$ which is cut by the node line either at $\chi=\pi/2$ (class A) or $\chi=\pi/4$ (class B for $\Delta_0^{(0)}=0$). In the former case the v_c component is large for the nodal plane at $\chi=\pi/2$ despite the fact that Bloch's theorem requires $v_c \equiv 0$ for quasiparticles in the Bragg plane. It is obvious that the Γ-centered FS model cannot correctly describe this case. This becomes clearer by looking at the true geometry of the major FS sheet in UPd_2Al_3 shown in the right part of Fig. 4 (full lines) which is a corrugated cylinder. As indicated by the arrows the quasiparticle velocity $\mathbf{v}=\hbar^{-1}\nabla_{\mathbf{k}}\varepsilon_{\mathbf{k}}$ is parallel to the Bragg plane for $\chi=\pi/2$ as it should be.

Therefore we conclude that the replacement of the corrugated cylinder by the Γ-centered cylinder FS is the source of the problem because it violates Bloch's theorem for quasi-

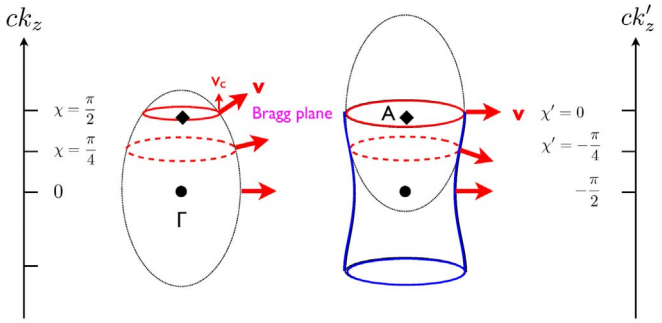

FIG. 4. (Color online) Two simplified FS models for UPd_2Al_3. Left: a Γ-centered ellipsoid FS. In this case quasiparticles in the $\chi=\pi/2$ line node of $\Delta_0 \cos k_z$ which is lying in the Bragg plane have a velocity component v_c perpendicular to the Bragg plane. This is not allowed by Bloch's theorem; therefore this FS model may not be used for calculating the thermal transport for this superconducting gap function. Right: the proper main FS sheet of UPd_2Al_3 is a Γ-centered corrugated cylinder (full line). For the quasiparticles in the node lines of $\Delta_0 \cos k_z$ ($\chi=\pi/2$) and $\Delta_0 \cos 2k_z$ ($\chi=-\pi/4$), this may locally be approximated by a shifted [Eq. (10)] A $(0,0,\pi/2c)$-centered ellipsoid (dashed line). Both the true and approximate FSs have $v_c=0$ for the node line $\chi=\pi/2$ ($\chi'=0$) of $\Delta_0 \cos k_z$, compatible with Bloch's theorem.

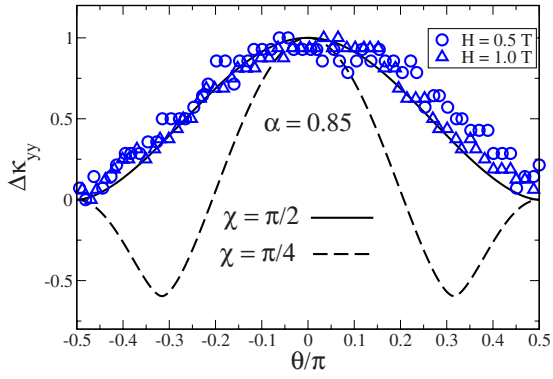

FIG. 5. (Color online) A comparison of the normalized thermal-conductivity calculations for $\Delta_0 \cos k_z$ (full line, $\chi=\pi/2$) and $\Delta_0 \cos 2k_z$ (dashed line, $\chi=\pi/4$) using the exact numerical integration of Doppler-shift expressions [Eqs. (4)–(6)]. Here the A $(0,0,\pi/2c)$-centered elliptical Fermi-surface model of Fig. 4 (right) is used. The symbols are the experimental results from Watanabe *et al.* (Ref. 19) (I). While the gap model $\Delta_0 \cos k_z$ ($\chi=\pi/2$ or $\chi'=0$) agrees with experimentally observed oscillations, the gap model $\Delta_0 \cos 2k_z$ ($\chi=\pi/4$ or $\chi'=-\pi/4$) leads to the wrong period of angular oscillations in $\Delta\kappa_{yy}(\theta)$.

particles on the $\chi=\pi/2$ node line and this has led to the spurious result for class A gap function (full line) in Fig. 3. This failure can be remedied in two ways. Firstly one may use the true corrugated cylinder Fermi surfaces as already suggested in (I) and used in explicit calculations in Ref. 21. This leads indeed to the proper behavior for the class A gap function, i.e., a monotonous decrease in $\Delta\kappa_{yy}(\theta)$ with increasing angle. Secondly, one may modify the present model calculation based on the simplified analytical treatment of Eqs. (4)–(6) which requires one to keep the elliptical FS model. For the comparison of different order-parameter models, it is not necessary to have a globally correct representation of the Fermi surface. It is, however, important that at the node lines of the order parameters considered the quasiparticle velocities of the true and approximated FS are close because they enter into the expression for the Doppler-shift energy $(m^*\mathbf{v}\cdot\mathbf{v}_s)$ which determines the angular oscillations of the thermal conductivity. For class A and B gap functions with $\chi=\frac{\pi}{2},\frac{\pi}{4}$, respectively, the true corrugated cylindrical FS may be well approximated by a shifted A-centered ellipsoid as shown in Fig. 3 (right, dashed line) where A $(0,0,\frac{\pi}{2c})$ is lying in the AF Bragg plane. For this shifted FS ellipsoid the quasiparticle velocities for the class A and B gap functions are well represented. For class A ($\chi=\frac{\pi}{2}$) we note that now $\mathbf{v}$ is parallel to the Bragg plane (no c component) as it should whereas for class B only the sign of the c component is reversed with respect to the Γ-centered FS (left, dashed line of Fig. 3). This does not influence the absolute DS which enters in the thermal conductivity. Therefore the results for class B will be the same as before but for class A it will be completely different. Technically the A-centered FS model may simply be implemented by the shift

$$\chi' = ck'_z = c\left(k_z - \frac{\pi}{2c}\right) = \chi - \frac{\pi}{2}, \tag{10}$$

which means that for class A: $\chi=\frac{\pi}{2c}\rightarrow\chi'=0$ and for class B: $\chi=\frac{\pi}{4c}\rightarrow\chi'=-\frac{\pi}{4c}$. To correct the previous analysis by using the proper Fermi-surface geometry, we therefore have to make this substitution in Eq. (6) for the Doppler-shift integrand. As explained above this will lead to a complete change in angular dependence of $\Delta\kappa_{yy}(\theta)$ for class A but no change for class B. The final correct result of the treatment using Eqs. (4)–(6) and using the proper A-centered FS [Eq. (10)] is presented in Fig. 5. It shows that (i) $\Delta_0 \cos k_z$ (class A node line $\chi=\frac{\pi}{2c}$) is in excellent agreement with the experimentally observed angular dependence of thermal conductivity. (ii) $\Delta_0 \cos 2k_z$ (class B, node lines $\chi=\pm\frac{\pi}{4c}$) can be ruled out because it predicts the wrong periodicity of angular variations in thermal conductivity.

VI. DISCUSSION

The conclusion drawn from the DS analysis presented here are in complete agreement with the qualitative arguments and proposals made in (I) but do not support those in (II). We have shown in detail how this discrepancy arose.

Because of an approximate Doppler-shift calculation in (II), it was not noticed that the class B gap function predicts the wrong periodicity. Furthermore due to a FS model which has a forbidden quasiparticle velocity component perpendicular to the Bragg plane, an upturn of thermal conductivity with increasing field angle θ for class A gap function was obtained. Together this has led to a conclusion on gap symmetry which is opposite to the correct one depicted in Fig. 5. Therefore as far as the DS analysis of thermal conductivity is concerned, $\Delta_0 \cos k_z$ agrees with experimental observation and $\Delta_0 \cos 2k_z$ may be ruled out.

A few words of caution are finally appropriate. The real strength of angle-resolved magnetothermal transport consists in its power to determine the node line *orientation* with respect to the crystal axes. This feature is based simply on the observation (or lack thereof) of thermal-conductivity oscillations for the appropriate geometry. This qualitative fact is already sufficient to rule out gap function candidates that have the wrong orientation of node lines, e.g., the one proposed in Ref. 40 for UPd_2Al_3. However, it is not sufficient to discriminate between different order parameters with the same node line orientation because both will lead to field-angular oscillations. Then a detailed comparative analysis of oscillations such as presented here is necessary. Naturally the conclusions may depend on the type or quality of approximations that have been used to calculate $\Delta\kappa_{yy}(\theta)$. The present approach, which was also used in (II), is based on a simplified analytical approximation based on the Doppler-shift theory for magnetotransport. The conclusions reached here are in complete agreement with those obtained by purely qualitative arguments in (I) (see Fig. 4 of this reference) which have been further substantiated by fully numerical treatment of Doppler-shift calculations of thermal conductivity[21] for the cylindrical FS model. Thus our present conclusions are consistent with the previous work. As a result the Doppler-shift analysis of thermal conductivity presented here forces us to reject the proposal of a $\Delta_0 \cos 2k_z$ gap function. An alternative to the low-field Doppler-shift method is the semiclassical treatment of thermal transport in UPd_2Al_3 which is in principle valid at larger fields. It was used in Ref. 41 and applied to the cylindrical FS model. The conclusions are somewhat different; it is mentioned there (but not shown explicitly) that all gap functions investigated exhibit either twofold or fourfold oscillation depending on whether the anisotropy parameter α is smaller or larger than the value used here.

It is now clear that a proper inclusion of the actual Fermi-surface properties is important for drawing the right conclusions from the angle dependence of the thermal conductivity. The latter is not directly a fingerprint of the nodal gap structure only. As we have shown one has to make sure that, for those gap models which are compared, the Fermi surface and quasiparticle velocities are realistically described, which should be obvious from the basic Doppler-shift energy expression. In particular the symmetry requirements on the direction of $\mathbf{v}$ resulting from Bloch's theorem have to be respected. Such a procedure is most easily followed when the Fermi surface is strongly dominated by one sheet, as is the case for the corrugated cylinder of UPd_2Al_3. For a material with a complicated many sheet Fermi surface the Doppler-shift model used here may be more difficult to employ but qualitative conclusions on the node line orientation can still be made.

VII. CONCLUSION

The symmetry determination of superconducting order parameters is a difficult problem, especially in cases such as heavy-fermion systems where direct methods such as angle-resolved photoemission spectroscopy are not applicable. The most powerful methods to date are the classical Knight shift and NMR relaxation studies, and more recent methods such as field-angle-resolved thermal conductivity and the observation of feedback resonance effects in inelastic neutron scattering. Usually the choices of gap symmetry are not unique and the issue has to be studied in detail until a consensus may be reached. The case of UPd_2Al_3 has special importance because it is the only heavy-fermion system where the pairing mechanism has been identified.[8,22] Therefore resolving the ambiguity that arose in (I) and (II) through the interpretation of thermal-conductivity measurements has been an urgent problem which we have resolved here.

Together, using the results of all methods cited above we conclude that beyond any reasonable doubt the superconducting gap function in UPd_2Al_3 is of class A, i.e., $\Delta_0 \cos k_z$ as proposed in (I), with possible admixture of higher harmonics as described in Eq. (2). This means that the node lines are lying in the AF Bragg planes $\chi=\frac{\pi}{2}$. This choice of the gap function is compatible with thermal-conductivity results, its nodal positions are required by the observation of an INS feedback resonance, and it is the natural outcome of microscopic theoretical models. Furthermore this superconducting state may easily coexist with the observed large moment background AF order. None of these conditions is fulfilled for the subsequently proposed $\Delta_0 \cos 2k_z$ gap function.

ACKNOWLEDGMENTS

One of us (P.T.) would like to thank Ilya Eremin for discussions. P.T. also would like to acknowledge hospitality of the Asia Pacific Center of Theoretical Physics in Pohang, Korea, where part of this work has been performed.

[1] V. P. Mineev and K. V. Samokhin, *Introduction to Unconventional Superconductivity* (Gordon and Breach Science, Amsterdam, 1999).

[2] P. W. Anderson, *Basic Notions of Condensed Matter Physics*, Frontiers in Physics (Benjamin, Menlo Park, 1984), Vol. 55.

[3] P. Thalmeier and G. Zwicknagl, *Handbook of the Physics and Chemistry of Rare Earths* (Elsevier, New York, 2005), Vol. 34, Chap. 219, p. 135.

[4] Y. Matsuda, K. Izawa, and I. Vekhter, J. Phys.: Condens. Matter **18**, R705 (2006).

[5] I. Eremin, G. Zwicknagl, P. Thalmeier, and P. Fulde, Phys. Rev. Lett. **101**, 187001 (2008).

[6] N. Bernhoeft, N. Sato, B. Roessli, N. Aso, A. Hiess, G. H. Lander, Y. Endoh, and T. Komatsubara, Phys. Rev. Lett. **81**, 4244 (1998).

[7] N. Bernhoeft, Eur. Phys. J. B **13**, 685 (2000).

[8] N. Sato, N. Aso, K. Miyake, R. Shiina, P. Thalmeier, G. Varelogiannis, C. Geibel, F. Steglich, P. Fulde, and T. Komatsubara,

Nature (London) **410**, 340 (2001).
[9] A. Hiess, N. Bernhoeft, N. Metoki, G. H. Lander, B. Roessli, N. K. Sato, N. Aso, Y. Haga, Y. Koike, T. Komatsubara, and Y. Onuki, J. Phys.: Condens. Matter **18**, R437 (2006).
[10] J. Chang, I. Eremin, P. Thalmeier, and P. Fulde, Phys. Rev. B **75**, 024503 (2007).
[11] O. Stockert, J. Arndt, A. Schneidewind, H. Schneider, H. S. Jeevan, C. Geibel, F. Steglich, and M. Loewenhaupt, Physica B **403**, 973 (2008).
[12] C. Stock, C. Broholm, J. Hudius, H. J. Kang, and C. Petrovic, Phys. Rev. Lett. **100**, 087001 (2008).
[13] W. Bao, P. G. Pagliuso, J. L. Sarrao, J. D. Thompson, Z. Fisk, J. W. Lynn, and R. W. Erwin, Phys. Rev. B **62**, R14621 (2000).
[14] G. E. Volovik, JETP Lett. **58**, 469 (1993).
[15] K. Izawa, H. Yamaguchi, Y. Matsuda, H. Shishido, R. Settai, and Y. Onuki, Phys. Rev. Lett. **87**, 057002 (2001).
[16] H. Aoki, T. Sakakibara, H. Shishido, R. Settai, Y. Onuki, P. Miranovic, and K. Machida, J. Phys.: Condens. Matter **16**, L13 (2004).
[17] A. Vorontsov and I. Vekhter, Phys. Rev. Lett. **96**, 237001 (2006).
[18] C. Geibel, C. Schank, S. Thies, H. Kitazawa, C. C. Bredl, A. Böhm, M. Rau, A. Grauel, R. Caspary, R. Helfrich, U. Ahlheim, G. Weber, and F. Steglich, Z. Phys. B: Condens. Matter **84**, 1 (1991).
[19] T. Watanabe, K. Izawa, Y. Kasahara, Y. Haga, Y. Onuki, P. Thalmeier, K. Maki, and Y. Matsuda, Phys. Rev. B **70**, 184502 (2004).
[20] H. Won, D. Parker, K. Maki, T. Watanabe, K. Izawa, and Y. Matsuda, Phys. Rev. B **70**, 140509(R) (2004).
[21] P. Thalmeier, T. Watanabe, K. Izawa, and Y. Matsuda, Phys. Rev. B **72**, 024539 (2005).
[22] M. Jourdan, M. Huth, and H. Adrian, Nature (London) **398**, 47 (1999).
[23] P. McHale, P. Fulde, and P. Thalmeier, Phys. Rev. B **70**, 014513 (2004).
[24] G. Zwicknagl, A. Yaresko, and P. Fulde, Phys. Rev. B **68**, 052508 (2003).
[25] P. M. Oppeneer and G. Varelogiannis, Phys. Rev. B **68**, 214512 (2003).
[26] H. Shimahara, Phys. Rev. B **72**, 134518 (2005).
[27] P. Thalmeier, Eur. Phys. J. B **27**, 29 (2002).
[28] Y. Inada, H. Yamagami, Y. Haga, K. Sakurai, Y. Tokiwa, T. Honma, E. Yamamoto, Y. Onuki, and T. Yanagisawa, J. Phys. Soc. Jpn. **68**, 3643 (1999).
[29] P. Monthoux and G. G. Lonzarich, Phys. Rev. B **63**, 054529 (2001).
[30] H. Tou, Y. Kitaoka, K. Asayama, C. Geibel, C. Schank, and F. Steglich, J. Phys. Soc. Jpn. **64**, 725 (1995).
[31] N. Bernhoeft, Eur. Phys. J. B **13**, 685 (2000).
[32] K. Miyake and N. K. Sato, Phys. Rev. B **63**, 052508 (2001).
[33] H. Won and K. Maki, arXiv:cond-mat/0004105 (unpublished).
[34] P. Thalmeier and K. Maki, Europhys. Lett. **58**, 119 (2002).
[35] A. V. Balatskii, L. I. Burlachkov, and L. P. Gorkov, Sov. Phys. JETP **63**, 866 (1986).
[36] L. N. Bulaevskii, Int. J. Mod. Phys. B **4**, 1849 (1990).
[37] J. Hessert, M. Huth, M. Jourdan, H. Adrian, C. T. Reick, and K. Scharnberg, Physica B **230-232**, 373 (1997).
[38] Y. Haga, E. Yamamoto, Y. Inada, D. Aoki, K. Tenya, M. Ikeda, T. Sakakibara, and Y. Onuki, J. Phys. Soc. Jpn. **65**, 3646 (1996).
[39] Y. Haga, H. Sakai, and S. Kambe, J. Phys. Soc. Jpn. **76**, 051012 (2007).
[40] Y. Nisikawa and K. Yamada, J. Phys. Soc. Jpn. **71**, 237 (2002).
[41] L. Tewordt and D. Fay, Phys. Rev. B **72**, 014502 (2005).